EXPERIMENTAL STUDY ON MECHANISM OF AUTOGENEOUS SHRINKAGE OF DIFFERENT TYPE OF SLAG CEMENT

Article · January 2009

1 author:

Januarti Jaya Ekaputri
Institut Teknologi Sepuluh Nopember
128 PUBLICATIONS   **564** CITATIONS

SEE PROFILE

Some of the authors of this publication are also working on these related projects:

Project   Synthesis and Characterization of Ni0.8Zn0.2Fe2O Nanoparticles by Self Combustion Technique View project

Project   Heavy metal immobilization by fly ash geopolymer View project

EXPERIMENTAL STUDY ON MECHANISM OF AUTOGENEOUS SHRINKAGE OF DIFFERENT TYPE OF SLAG CEMENT

Januarti Jaya Ekaputri

Abstract: *A caution procedure to use embedded sensor to measure internal RH and shrinkage of mortar with low W/C ratio was proposed in detail in this paper. Mortar specimens made from seven slag cements were prepared with the same mix proportion and cured under a sealed condition at 20°C. The results were then compared with the shrinkage of OPC mortar and the one made with 40% BFS replacement. The results showed higher shrinkage and greater moisture consumption when BFS was introduced to OPC and a great scattered throughout the shrinkage deformation occurred at the specimen from slag cement type B. Compressive strength and autogeneous shrinkage were analyzed at a certain age. A linear relation between the autogeneous shrinkage and the compressive strength of slag cement mortar was obtained. The slag content, the creation of the early hydrated products, the greater chemical shrinkage, pore structure of blended cement, chemical composition and the particle shapes were thought to be the main factor of the shrinkage magnitude.*

Key word: Autogeneous shrinkage, BFS; type B; embedded sensor, internal RH

1. Introduction

An indecisiveness of using BFS in concrete, particularly its application at low W/C ratio, is necessary to be investigated through a comprehensive study. The mechanical stability of concrete is affected by shrinkage, especially if they contain supplementary cementitious material such as fly ash or slag (**Kanna, 1998**). This composite cement in industrial application is known as blended cement. It is reported that its properties improve slowly in comparison with ordinary Portland cement (OPC). The hydration rate of this supplementary material is less reactive. Therefore, inadequate water supply in the mixture or water that evaporated from the product at the early age results in lower performance. It is well known that the moisture content at early ages generally plays an important role to the shrinkage of cementitious material. A large shrinkage induces micro-crack formation resulting in strength reduction.

Moreover, it was reported that autogenous shrinkage of concrete increases when cement containing BFS is applied in the low water to cement ratio mixtures (Tazawa, 1994). Low water to cement ratio will promote the mixture to self-desiccate due to inadequate water in hydration reaction. The issue about autogenous shrinkage becomes an important factor concerning early ages cracking control in concrete with low water to cement ratio. The shrinkage caused by volumetric changes induces cracking in early ages. The cracks are considered to be a serious problem in concrete durability. In a large application of cement composite with BFS when it is used in a massive application for large-scaled of structural members in the field, the cracks are considered for structure's useful life. When there is no movement in concrete mass, under a restrained condition, developing of residual stress induces early age cracking potential of the structure. The increase of autogeneous shrinkage is also promoted by higher percentages of cement replacement by the slag.

The purpose of this paper is to investigate autogenous shrinkage of mortar using different slag cements, which can be categorized in slag cement type B. The slag cements are specified in JIS R 5211 that contain 30% to 60% of slag. In this paper, specimens adopted from 7 slag cements were prepared by mortar with W/C ratio of 35% and cured at temperature of 20oC and RH of 60%. At the same condition, the results were then compared with the shrinkage of OPC mortar and the one made with 40% BFS replacement into cement weight. Compressive strength of each specimen was then plotted to the shrinkage at a certain age. The effect of internal RH on low W/C ratio and BFS application were also considered in this paper to investigate the moisture consumption at early ages. It will be shown that using BFS in mortar mixture leads lower internal RH and higher autogeneous shrinkage as compared to OPC cement.

* Corresponding author: januarti@ce.its.ac.id

Civil Engineering Department, ITS, Surabaya

Finally, this paper provides a discussion about influential factors to deal with shrinkage problems regarding the application of slag cement in the mixture. A comprehensive benchmarking was considered on the slag content in the mixture, the particle size distributions, chemical properties of cement slag and the fact that slag varies in reactivity. The main results reported here are associated with the main goal of this study for massive application of by-product in the field.

2.   Materials Properties and Mix Proportion

(1) Physical and chemical composition of cements

To investigate the internal moisture, an ordinary Portland cement (OPC) with chemical composition as shown in **Table 1** was used. Some specimens were prepared to contain 40% of cement weight partially replaced with BFS. Physical properties of OPC and BFS are listed in **Table 2**. Seven slag cements in this paper were adopted for autogeneous shrinkage measurement and subsequently coded as A, B, C, D, E, F, and G. Physical properties and mineral composition of slag cements are listed in **Table 2** and **Table 3**.

Table 1 Chemical composition (%)

Code	SiO$_2$	Al$_2$O$_3$	Fe$_2$O$_3$	MnO	CaO	MgO	SO$_3$	f-CaO	Ig. loss
OPC	21.36	5.28	2.66	n/a	65.02	1.46	2.08	n/a	1.77
A	26.27	9.70	1.93	0.13	55.00	3.32	1.76	0.20	0.38
B	24.74.	9.27	2.03	0.12	55.44	2.83	1.90	0.33	2.27
C	25.96	9.27	1.76	0.15	54.54	3.19	2.11	0.16	1.40
D	24.05	8.94	2.11	0.13	54.45	3.32	2.35	0.32	2.04
E	25.71	9.61	1.79	0.12	54.41	3.41	1.90	0.37	1.49
F	26.17	9.92	1.61	0.07	54.06	3.13	1.96	0.43	1.62
G	27.31	10.98	1.44	0.21	49.22	4.41	3.35	0.27	0.99

Table 2 Physical properties of cements.

Code	Density (g/cm^3)	Blaine surface area (cm^2/g)	Average Particle size (μm)	Particle width dist. (N)
OPC	3.16	3480	n/a	n/a
BFS	2.88	4100	n/a	n/a
A	3.06	4000	14.5	0.99
B	3.05	3630	16.8	1.08
C	3.02	3750	16.0	1.03
D	3.04	3880	13.7	0.97
E	3.04	4150	14.9	1.01
F	3.01	3790	15.9	0.98
G	2.98	3380	16.2	0.95

According to the data sheet of each material, Rietveld method **(JSCE, 2010)** was used for mineral composition of all slag cements. Slag cements A, B, C, D, E, F, and G can be categorized as slag cement type B as their slag content is in the range from 30% to 60%.

Table 3 Mineral composition (%)

Code	C3S	C2S	C3A	C4AF	BFS	Lime	MgO	Gyp	Calcite
OPC	53.21	20.81	9.76	8.51	-				
A	66.2	10.9	4.8	11.4	42.2	-	0.6	0.5	-
B	58.6	10.4	7.1	11.1	41.1	-	0.5	2.4	5.4
C	62.6	10.1	5.2	10.7	41.7	-	0.6	2.9	3.7
D	58.6	10.2	5.1	11.7	37.4	0.1	0.6	1.0	4.0
E	53.2	16.5	9.5	10.4	48.4	-	-	3.2	2.7
F	59.6	13.7	5.7	10.2	42.5	-	0.1	2.9	3.2
G	53.3	6.4	6.5	10.5	55.7	-	0.6	1.8	3.7

(2) Mix proportion of specimens

Mortar specimens made with OPC, and OPC replaced with BFS were prepared to have W/C ratio of 35% and 25%. The specimens with W/C ratio of 35% were then adopted as the control system of seven slag cements for autogenous shrinkage measurement. Mix proportion of each specimen is listed in **Table 4**. The compositions included the use of a superplasticizer from SP8SBS of 0.55% cement weight to aid the workability of fresh mortar. Sand with a density of 2.63g/cm^3 was applied as the fine aggregate with 40% volume.

Table 4 Mix proportion of specimen

Code	W/C (%)	Cement kg/m^3	Water kg/m^3	Sand kg/m^3	SP kg/m^3	BFS kg/m^3
OPC −25%	25	995.70	248.90	988.88	14.90	0
OPC+BFS −25%	25	597.40	248.90	988.88	11.90	398.30
OPC−35%	35	846.27	296.19	988.88	4.65	0
OPC+BFS −35%	35	507.76	296.19	988.88	4.65	338.51
A	35	833.34	291.67	988.88	4.58	0

B	35	832.02	291.21	988.88	4.58	0
C	35	828.04	289.81	988.88	4.55	0
D	35	830.70	290.74	988.88	4.57	0
E	35	830.70	290.74	988.88	4.57	0
F	35	826.71	289.35	988.88	4.55	0
G	35	822.67	287.94	988.88	4.52	0

Compression test to obtain the strength of some specimens at 1, 3, 7, 14, and 28 days was conducted according to **JIS A1108**. An average from 3 identical specimens was determined for each variation of specimens made with slag cements and OPC. Each specimen with 35% of W/C ratio was cured under a sealed condition at a controlled condition chamber until loaded in compression at the specified age.

3.   Relative Humidity Measurement

This measurement is used to investigate the effect of W/C ratio and BFS application on moisture consumption at very early age. Mortar specimens with W/C ratio of 25% and 35% were prepared as shown in **Table 4**. Based on a method proposed by **Grasley (2002)**, which can successfully measure internal RH of OPC mortar with embedded sensor, a proposed method for BFS mortar is applied in this study. In this paper, problems occurred when the sensor was applied to the mixture of mortar incorporating BFS was solved. Non-avoidable vapor containing chemical product during early hydration deteriorates the sensors and makes inaccurate measurement. For this reason, the problem was then investigated considering usability of the sensor and housing for sensor. This issue is avoided by putting the sensor into concrete after it set. This method was conducted by inserting the sensor directly into the measuring point after the concrete is sufficiently hardened by providing inserting path (pre-embedded pipe) before casting. The following is the step to install the sensor.

(1) Pipes and Molds Preparation

This experiment was conducted at a sealed condition under room temperature at 20°C and a constant 60% of RH. Cylindrical molds with diameter 10 cm and 20 cm in height are used for internal RH measurement. An acrylic pipe with an inner diameter of 11 mm is fixed by two small wires at the center of the mold by making two small holes in the mold. One end of the pipe is wrapped whit waterproof/breathable fabric (Gore-Tex) made from polytetrafluoroethylene (PTFE). It will allow vapor from mortar to be captured by sensors but prevent the hydration products reaching the sensors during the hydration process. A rubber cap is inserted

through the pipe until an end to prevent vapor flow into the pipe during casting as shown in **Figure 1**.

wrapping with plastic
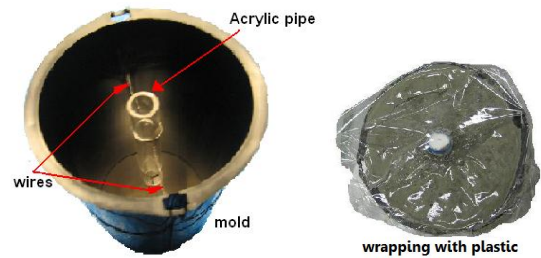
Figure 1 Acrylic pipe was set at the center of mold and prevented from mortar.

(2) Inserting RH Sensors

The sensor is sealed surrounding also by rubber on its cable to prevent vapor loss at the measuring point. After 6 to 12 hours, depends on setting time of specimens, the rubber is replaced by RH sensor immediately not to disturb moisture equilibrium inside the pipe. After that, silicone is filled in the empty space to make sure that vapor from mortar cannot escape during measurement. To obtain a higher accuracy measurement, two sensors can be located in the center of mold. An average value will be obtained from two readings. Then, measurement can be monitored as shown in **Figure 2**.
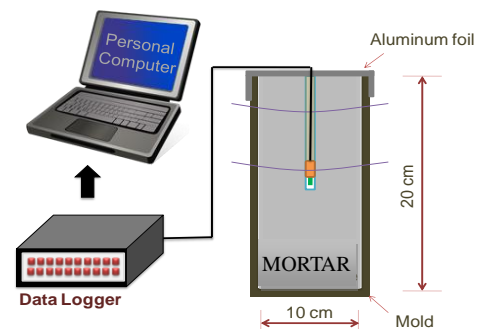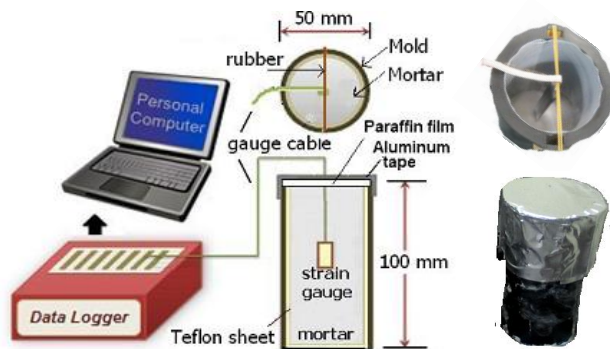

Figure 2 the setting of internal RH measurement

The experimental results were then compared with the analytical ones by the thermo-hygro simulation system named *DuCOM*, which has been developed in author`s research group (**Maekawa, 1999**). The finite element mesh for specimen with 1/12 cylindrical model was used in simulation. It has the same geometric conditions, mix proportions, and the atmospheric condition as those used in the experiment.

4.   Autogeneous Shrinkage Measurement

The autogenous shrinkage of mortar specimens in this paper was measured according to a method proposed by **Nawa et al. (2004)**. This measurement is used to investigate the effect of W/C ratio and BFS

application in mixture for OPC mortars and the influential factors for different magnitude of slag cement shrinkage. Mortar specimens are made with W/C ratio of 25% and 35% for OPC mortars. Then, the result from specimens made with W/C ratio of 35% was used as a control system for slag cement mortars with mix proportion in **Table 4**. The measuring method of autogenous shrinkage strain and temperature of specimens is shown in **Figure 3**. Free autogenous shrinkage strain of mortar under sealed curing conditions from specimens listed in **Table 4** was measured by embedded gauges. A 70 mm long thin strain gauge, having thermocouple and covering with waterproof silicone was equipped. Specimen used in this measurement was cast in a cylindrical mold of 5 cm in diameter and 10 cm in length. A teflon sheet was placed between the mold and the mortar in order to allow it shrink freely. In this study, the measurement of autogenous shrinkage is conducted by measuring the change in linear length of the specimen. Then, the strain gauge was placed vertically at the center of the mold and hanged on its cable with a rubber. After fixing the gauge at the center of the cylindrical mold, the mold was then filled with the fresh mortar. In order to prevent evaporation of moisture to the surrounding, the top surface of the specimen was sealed using a paraffin film and wrapped with aluminum foil sheet. Afterward, all specimens were kept in an environmental control room at a constant temperature of 20°C and constant humidity of 60%. Finally, immediately after mixing, the change in strain was continuously measured and recorded by a personal computer. An average value from 3 specimens in the same condition and mixture was obtained.

surrounding the gauges. An air-dried gauge from it package can easily absorb moisture from the specimen paste that causes the gauge showing a striking expansion of the mortar. To put it more simply, the gauges will not be ready to use until a stable condition is reached at 3 weeks in immersion when the gauges are saturated and stops absorbing water from the surrounding environment.

5. Reliability and Reproducibility

Each specimen was applied with a gauge and repeated for 4 times by using the same method. As a result, the strain of different gauge recorded from each measurement. **Figure 4** shows the shrinkage measurement against time curves for four parallel measurements. The similarity of the four curves verifies that the measurement method has a good reproducibility.

Figure 4 Reproducibility check on four measurements

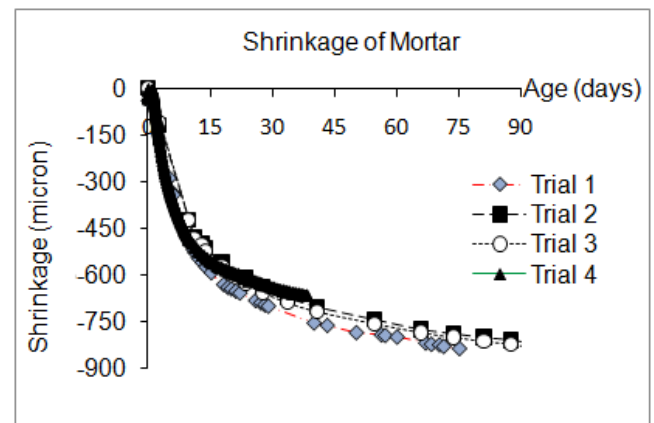**Figure 3** The proposed experiment set up.

The application of pre-embedded gauges to measure autogeneous shrinkage of mortar, needs pre-treatment as a principal part of the overall process. An elaborate investigation was then proposed for reliability measurement.

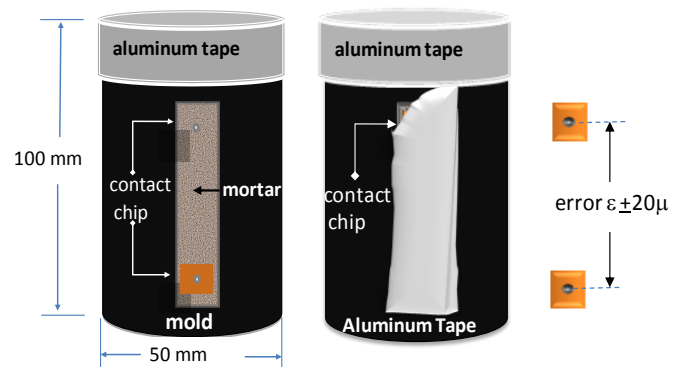Catalogue product of the gauges informs that gauges are affected by the moisture conditions

Figure 5 Shrinkage measurement with contact gauges

A mechanical measurement method was adopted as a comparison for the reliability result. A pair of contact chip was used as a mechanical strain gauge.

To start with, three identical specimens using OPC mortar without any embedded gauge were prepared, sealed and stored in the controlled chamber at a normal condition. Next, a vertical streak was made to put two contact chips in a stripe on the mortar surface. Then the distance between two contact chips was set as a reference point for the next measurement. Afterward, the hole was covered with an aluminum tape to ensure a sealed condition as shown in **Figure 5**. The tape was opened only for measurement at once a day.

Thus, the strain measured with this method was compared with the one from embedded gauges as plotted in **Figure 6**. Comparatively, the difference shrinkage between contact gauges and embedded gauges was only up to 50μ.
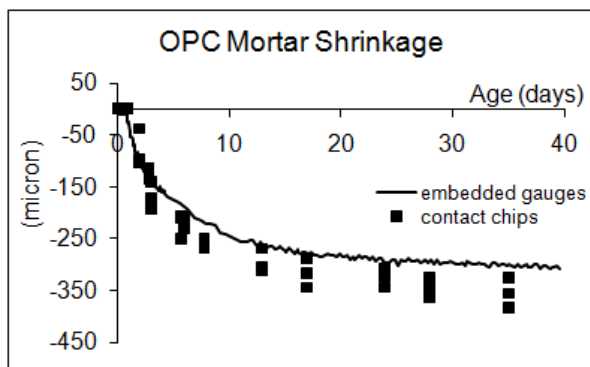
Figure 6 Comparison results of shrinkage between embedded and contact gauges

6.   Discussions

(1)   Internal Relative Humidity

 (a)   The effect of water to binder ratio

The internal RH measurement result in the specimen due to self-desiccation is shown in **Figure 7**.
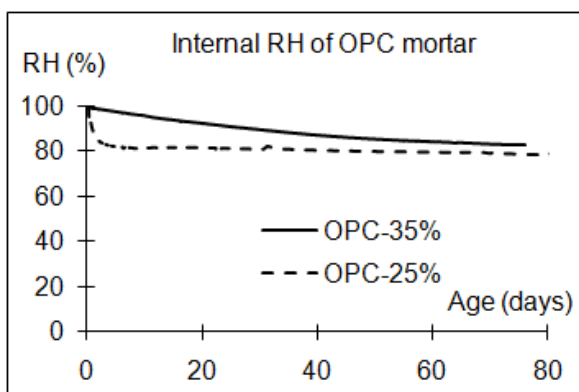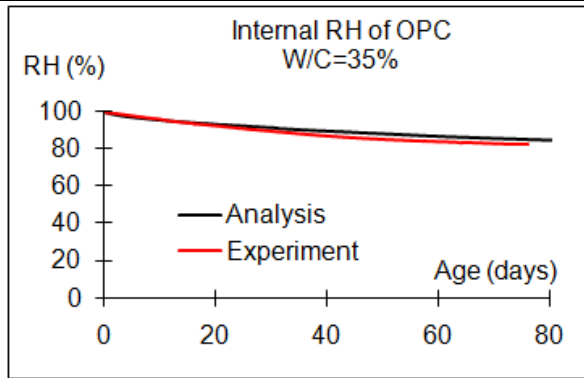

Figure 7 Internal RH comparison for OPC specimen

The pores were more saturated at the start of the experiment in specimen with W/C ratio of 35% than that with W/C ratio of 25%. Internal RH of sealed OPC mortar with W/C ratio of 25% decreases to 78% at 80 days while at W/C ratio of 35% it only decreases to 82%. It indicates that more internal moisture decreased by self-desiccation as a decrease of the water to cement ratio, especially at early ages due to denser pore structure. **Figure 8** illustrates the same trend when the mortars contain BFS. The lower W/C ratio is, the higher the self-desiccation results to impact decreasing of internal RH of mortars.

The analytical results of RH distribution obtained from experimental results for specimens with W/C ratio of 35% were then compared by the analytical results by using *DuCOM*. It is an integrated computational system designed based on physical and thermodynamics theories to evaluate durability performances since cement comes into contact with water. *DuCOM* is a versatile program for cementitious material and applicable to application of fly ash, BFS concretes, and, etc. in mixtures. Experiments verified that this computational system can accurately predict hydration processes and relative humidity for a different mix proportions under various temperatures (**Ishida, 2007**). The input data used in the analytical program such as the geometric conditions, mix proportions, and the atmospheric condition is the same as those used in the experiment. According to the comparison shown in **Figure 9**, the experiment result agrees with the analytical result.
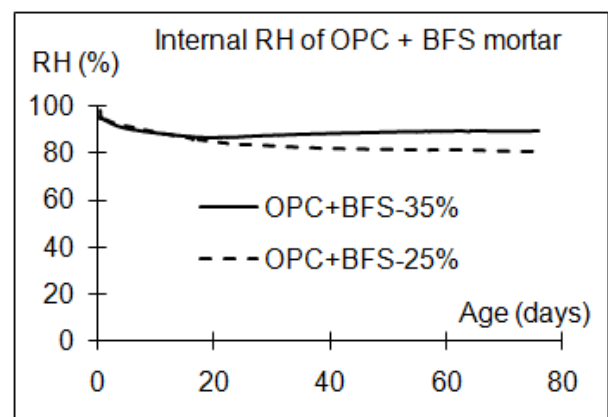
**Figure 8** Internal RH of OPC mortar containing BFS.

Figure 9 IRH Comparison of analytical and experimental results

(b) The effect of Blast Furnace Slag (BFS)

In **Figure 10**, at the same W/C ratio given, internal RH decrement of OPC specimen incorporated with 40% BFS is higher than that of pure OPC specimen at the same ages. Higher chemical shrinkage of cement containing BFS might lead to greater self-desiccation, since there is no water supply under sealed curing. If the water supply is restricted, pores empty and air-water menisci form (**Lim and Wee, 2000**). Here, moisture consumption in specimen containing BFS is faster than that in pure OPC specimen. Under the same condition, hardened OPC mortar with more fine pores tends to retain more water, while higher water loss might be contributed by the coarser pore structure of BFS mortar at very early age.

Fineness of BFS is also considered as mechanical accelerator (**Roy and Idorn, 1982**). As BFS has finer particles, which has larger surface area, it increases both the pozzolanic reaction and the water consumption. It reduces pore sizes in cementitious matrix. This finer structure which is the product of the dissolution of the Calcium Hydroxide crystals and the precipitation of CSH produced by the pozzolanic reaction may cause the pores filled up. Those finer pores lead internal RH decrease very fast.
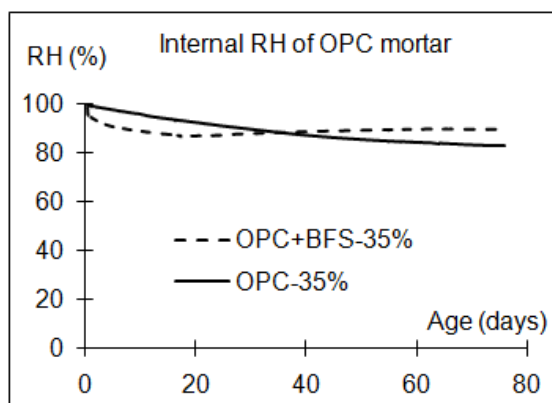

Figure 10 Internal RH of mortar with W/C ratio of 35%

(2) Autogeneous shrinkage

Autogeneous shrinkage-time curve from specimens with W/C ratio of 35% and 25% is presented in **Figure 11**. As predicted and indicated with internal RH experiment, specimens made with OPC with W/C ratio of 25% exhibit shrinkage two times larger than those specimens made with W/C ratio of 35%. This deformation occurs due to self-desiccation at early ages. The effect is more obvious for specimen containing BFS with lower W/C ratio.
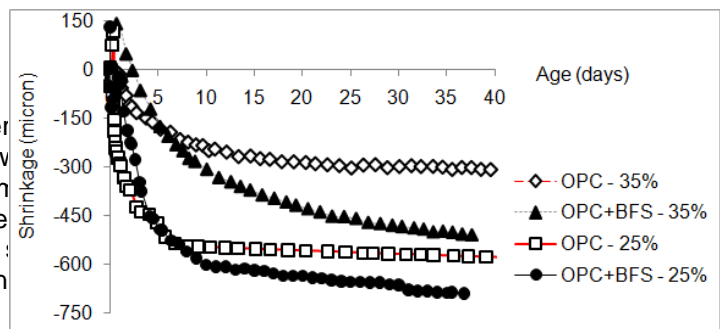
Figure 11 Autogeneous shrinkage of OPC and OPC containing BFS mortar resulting with changing W/C ratio
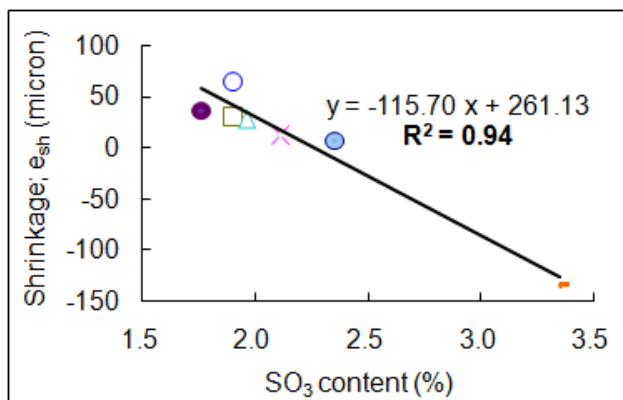
At the same W/C ratio, specimens containing BFS show higher shrinkage than that made with pure OPC. The increase of autogeneous shrinkage in mortar containing BFS is generally believed due to the alkali hydroxide reaction during early hydration which is followed later by pozzolanic reaction that fills up pores and gradually increases the strength (**Holt, 2005**). In the fine pores, water meniscus is created to induce large capillary pressure that results greater autogeneous shrinkage. Development of compressive strength of mortar containing BFS is slower than OPC mortar due to slower hydration reaction in capillary pores that causes the shrinkage deformation continues at later age.

The autogeneous shrinkage curves of slag cement during the first week are represented in **Figure 12**. It is interesting to recognize that gypsum content in slag cements leads to initial swelling of shrinkage just after casting. It can be seen that this expansion occurs at the beginning and then the strain gradually decreases due to the effect of self-desiccation. This swelling deformation was also reported by **Barcelo (2005)**. It can be seen from **Table 3** that specimen G has higher sulfate in the form of gypsum, hemi-hydrate and anhydrate, which control cement set.
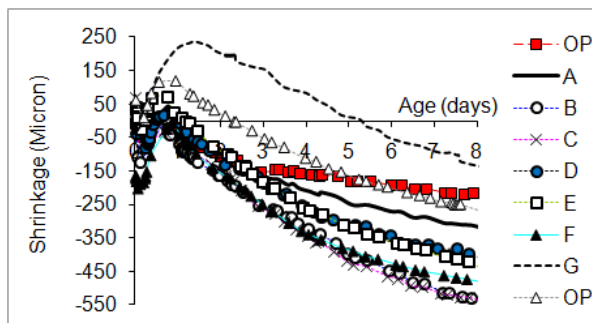
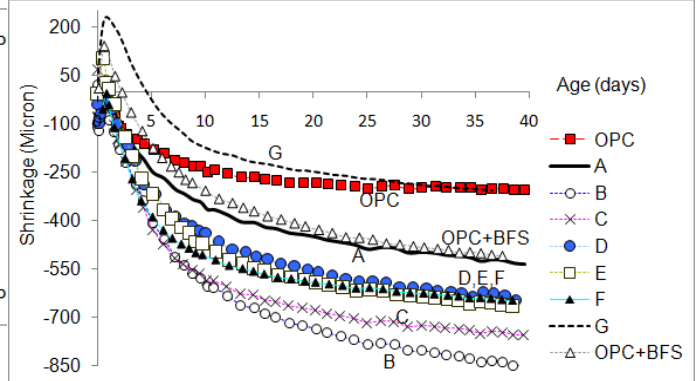**Figure 12** Mortar shrinkage at age 8 days

Figure 14 Shrinkage of specimens at 40 days

Harada (2003) furthermore, reported the effect of SO_3 to induce the expansion of cement paste deformation at early ages when it contains SO_3 more than 2%. The effect of SO_3 to the shrinkage just one day after casting is represented in **Figure 13**. It is also not surprising then, that the effect of sulfate content in slag promotes its expansion deformation at early ages obtaining small shrinkage at later age.

Figure 13 The effect of SO_3 content on autogeneous shrinkage at age 1day

Figure 14 shows the effect of exposure age to 40 days of mortar shrinkage. The rate of shrinkage deformation in slag specimens is higher than that in OPC. It also can be seen that introducing BFS as 40% of cement replacement leads higher shrinkage deformation at the extended time. A big magnitude is obviously shown by specimen made with slag cement type B. Specimen A exhibits deformation of -535 micro-strains at 40 days while Specimen B gives -850 micro-strains at the same age. Shrinkage deformation of specimen B is about three times larger than that of specimen made with pure OPC.

There are some factors, which affect the variation of the shrinkage values of slag cement type B. Physical and chemical properties play an important role. Average particle size and particle width distribution referring to **Table 2** contribute a factor to lead greater shrinkage. The higher value N (Rosin-Rammler`s value) represents cement particle size becomes uniform. On this basis, it can be inferred that specimen B, C, and E show higher shrinkage deformation than other slag cement mortars. **Figure 15** shows a linear relation between N and autogeneous shrinkage. The effect of N value starts from the first week and becomes stronger at 21 days. In general, the particle size of slag cement mortar does not have large difference. Specimen B, which has the smallest average particle size, shows higher shrinkage than specimen A. It means, the uniformity of particle size, denoted by N value, plays an important role to promote higher shrinkage.

It is often argued that chemical content in slag cement is one of the main factors to greater shrinkage at the early ages. Calcite ($CaCO_3$) content, for an example, as shown in **Table 3** is also deliberate to promote shrinkage deformation higher than the control system. It can be seen from the table, specimen B has the highest amount of calcite and the most uniform size of particles. It is possible that specimen B shows the greatest shrinkage deformation. On the other hand, specimen A does not contain calcite and has relatively broadened particle distribution. As a consequence, its shrinkage deformation is the smallest. The effect of $CaCO_3$ content on autogeneous shrinkage of specimens starts strongly from the first week as plotted in **Figure 16**.

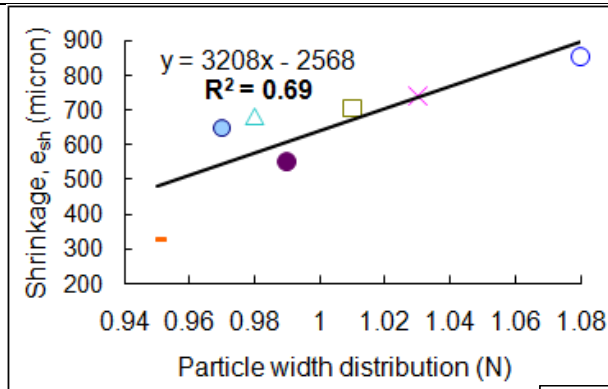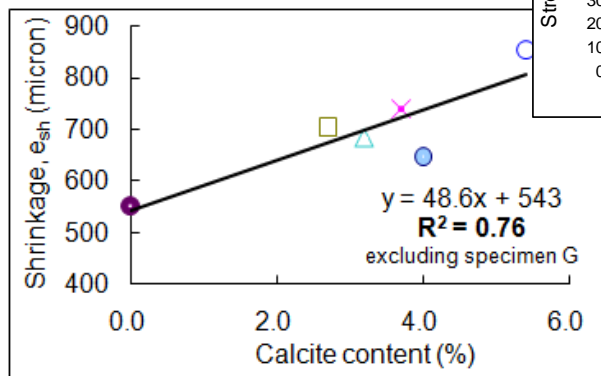**Figure 15** The effect of N value on autogen shrinkage at age 21 days

Figure 16 The effect of CaCO$_3$ on autogeneous shrinkage at age 7days

Dense pores contribute strength development but less hydration degree gives results in less strength development. Generally, the internal pores are gained when hydration product fills in the capillary pores. The rate of this mechanism is lower at early age. Thus, in this stage, different pore structures in the matrix due to different hydration mechanism are subjected not only by variation of mineral compositions but also different physical properties. This different mechanism causes the value vary in compressive strength.
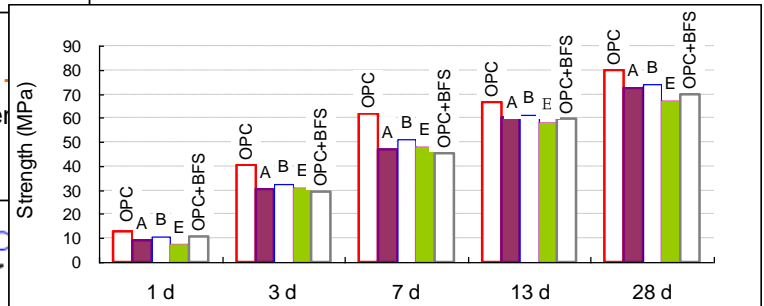

Figure 17 Compressive strength of slag cement and OPC mortar

(4) Shrinkage and strength relation

Figure 18 shows a relation between compressive strength and shrinkage at age 1d, 3d, 7d, 14d, and 28d. A linear relation is expressed by all specimens. The slope of the control system is different from slag cement caused by fewer shrinkage deformations. Surprisingly, when 40% cement weight is replaced with BFS, the slope changes to the same direction with slag cements.

(3)   Compression Test

From shrinkage measurement, the lowest shrinka deformation is contributed by specimen from sl cement A. Slag cement D, E, F, and G have modera deformation and finally slag C and B show the great shrinkage. Then, specimen A, E and B was adopt for compression test and compared to specime made with OPC and OPC introduced with BF Compressive strength of specimens from 5 r proportions is plotted in **Figure 17**. Every r proportion shows different compressive strength ev the curing condition is the same. Among the slag cement specimens, the highest early strength is given by specimen B while E shows the lowest strength rate.

According to a research reported by **Taylor (1990)**, to insure higher early strength, usually cement containing a great amount of slag was produced with higher fineness. It is found that at early age, cement containing BFS with high replacement ratio gives denser pores but lower rate in hydration degree.
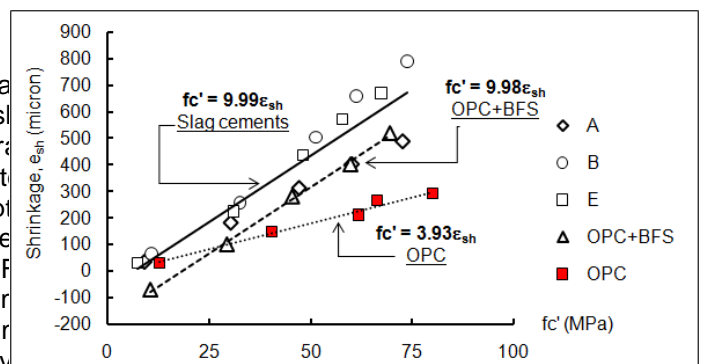

Figure 18 Linear relation between fc' and shrinkage of mortars

It is evident that strength development at early ages has a close relation with the porosity. The volume changes as solid formation from hydration products in the initial capillary space indicates the strength development. The characteristics of these hydration products are also represented by the type of the origin

141

minerals of cement clinker. The more capillary space is occupied with the hydration products, the higher compressive strength will be achieved. This can also explain the different strength given by each specimen at the same age.

At the later ages, gradually the progression of the hydration process generates finer gel pores developing continuously. In case of this low water to binder ratio, self-desiccation occurs. Internal RH in the capillary pores continues to decrease and then promote driving forces. The driving forces are believed to induce an additional stress for shrinkage deformation. The slopes presented by the shrinkage-fc' relation at slag cement specimens are different from the slope of OPC specimens. The steeper slope of slag cement specimens indicates their different pore size as a consequence of finer cement size particle, mineral content and chemical compound, which are involved in the hydration process.

7.   Conclusions

(1) Through a comprehensive experiment, this paper has shown the reliability of embedded sensors application for internal RH and shrinkage deformation measurement from very early ages of mortars made from slag cements. Preparation of material, pretreatment of equipments, and selection of appropriate sensors are important to obtain the accurate results.

(2) In this paper, a method proposed is concerned to study the effect of W/C ratio and BFS in the mixture on moisture distribution and autogeneous shrinkage. It was revealed that decrement of internal RH in mortar specimens at a low W/C ratio depends on moisture diffusion and self desiccation that induces autogeneous shrinkage. Finally, it was shown that using BFS in mortar mixture leads lower internal RH and higher autogeneous shrinkage in comparison to the one made with pure OPC cement. Physical and chemical properties of BFS are believed as the reason. Water consumed caused by finer particles and the chemical reaction at the early ages to start the hydration process may cause the lower moisture which leads to greater autogeneous shrinkage.

(3) The mortars made with slag cement type B with W/C ratio of 35% exhibits the large magnitude of autogenous shrinkage. At the exposure age, the rate of shrinkage deformation of specimens made with slag cement type B is higher result in greater deformation as compared to OPC with the same W/C ratio. It might be due to the creation of the early hydrated products, the greater chemical shrinkage, finer pore structure of the mortar containing BFS, and the particle shape of BFS. It is clear that this shrinkage mechanism cannot be only explained through the physical mechanism of self-desiccation that is induced by hydration.

(4) The maximum shrinkage deformation in the slag cement mortars is about three times larger than that of the OPC mortar. It can be decreased by longer and proper curing of specimens at the higher moisture condition, modifying the initial geometry of the cement particles, controlling the mineral composition and admixtures and also considering the application of high volume of BFS in cement.

(5) A linear relation between compressive strength and autogeneous shrinkage is shown by of all mortars. The steeper slope of slag cement specimens is due to higher shrinkage deformations. It indicates their different microstructure as a result of different size particles, mineral content and chemical compound, which are involved in the hydration process.

8.   References

1   Barcelo, L., Moranville, M. and Clavaud, B. (2005). "Autogenous Shrinkage of Concrete: a Balance between Autogenous Swelling and Self-desiccation". *Cement and Concrete Research*, 35, 177-183.

2   Grasley, Z.C and Lange (2002). "Modeling Drying Shrinkage Stress Gradients in Concrete". *Journal of Testing and Evaluatio*n.

3   Harada, Katsuki and Matsushita, Hiromichi (2003). "Effect of Gypsum Content in Cement on Autogeneous Shrinkage of Low-Heat Portland Blast-Furnace Slag Cement Concrete". *Memoirs of the Faculty of Engineering, Kyushu University*, Vol. 63, 1.

4   Holt, Erika (2005). "Contribution of Mixture Design to Chemical and Autogeneous Shrinkage of Concrete at Early Ages. *Cement and Concrete Research, vol 35, 464-472.*

5   Ishida, T., Maekawa, K. and Kishi, T. (2007). "Enhanced Modeling of Moisture Equilibrium and Transport in Cementitious Materials under Arbitrary Temperature and RH History". *Cement and Concrete Research, vol. 37, 565-578.*

6   Kanna V., Olson R. A. and Jennings H. M. (1998), "Effect of shrinkage and moisture content on the physical characteristics of blended cement mortars", *Cement and Concrete Research, 28, 1467-1477.*

7   JIS A 1108:2006, "Method of Test for Compressive Strength of Concrete"

8   JIS R 5210:2003, "Portland cement"

9   JSCE (2010). "The Investigation of Properties and Performance of Concrete with Supplementary Cementitious Materials". *Concrete Engineering Series, 309-310 (in Japanese).*

10 Lim S.N. and Wee T.H. (2000). "Autogeneous shrinkage of ground-granulated blast-furnace slag concrete". *ACI Materials Journal, 97, 587-593.*

11 Maekawa, K., Chaube, R.P. and Kishi, T. (1999). "Modeling of Concrete Performance". *E and FN SPON.*

12 Nawa, T. and Horita, T. (2004). "Autogenous Shrinkage of High-Performance Concrete".

Proceedings of the International Workshop on Microstructure and Durability to Predict Service Life of Concrete Structures, Sapporo, Japan.

13 Roy D. M. and Idorn G. M. (1982). "Hydration, structure, and properties of blast furnace slag cements, mortars and concrete". *ACI Journal, 444-457.*

14 Tazawa, E. and Miyazawa, S. (1994). "Influence of Cement and Admixture on Autogeneous Shrinkage of Cement Paste". *Cement and Concrete Research, vol.25, 2, 281-287.*

15 Taylor H. F. W. (1990). "Cement Chemistry," *Academic Press, London, 261-270.*